$K_1 = 0.4$, the expected ω-β diagram calculated from (2) is shown in Fig. 2. Since βL is a known function of ω in a given structure, the ordinate of Fig. 2 could have been plotted in terms of ω.

Consider now the situation when the far end of the periodic structure is shorted at P_2. The impedance seen by the input line at P_1 is obtained from the results of Slater

$$Z_{in} = jZ_0 \frac{\sin \beta L}{\sin \beta_0 L} \tan 5\beta_0 L, \qquad (4)$$

where the term

$$Z_0 \frac{\sin \beta L}{\sin \beta_0 L}$$

is the image impedance of the loaded line. Substituting the values of $\beta_0 L$ given by (2) and Fig. 2 into (4) would give the variation of Z_{in} with changes in βL. The null positions in the input line can also be expressed in terms of these values of Z_{in} as follows. The reflection coefficient "seen" by the input line at P_1 is

$$K_r = \frac{Z_{in} - Z_0}{Z_{in} + Z_0}$$

or from (4)

$$K_r = 1 \angle \pi + 2 \arctan \left(- \frac{\sin \beta L}{\sin \beta_0 L} \tan 5 \beta_0 L \right). \qquad (5)$$

A null occurs on the input line at a distance S from the point P_1, where

$$-\frac{2S}{\lambda}(2\pi) + 2 \arctan \left(- \frac{\sin \beta L}{\sin \beta_0 L} \tan 5\beta_0 L \right) = 0$$

or

$$\frac{S}{\lambda} = \frac{\arctan \left(- \frac{\sin \beta L}{\sin \beta_0 L} \tan 5\beta_0 L \right)}{2\pi}. \qquad (6)$$

If the values of S/λ given by (6) were plotted against βL, choosing the solution whose magnitude was less than $\frac{1}{4}$ each time, the cross-over points where $S/\lambda = 0$ would give the frequencies where $5\beta_0\lambda = n\pi$. These would correspond to $\beta_0 L = 0$, 0.2π, 0.4π, 0.6π, 0.8π, and 1.0π in the example under consideration.

In an experimental procedure, reference nulls which were a multiple of $\lambda/2$ away from P_1 would be taken and the motion of the nulls of the circuit under test about these would be observed. Fig. 3 shows the expected curves for the example under consideration when the reference null is taken $\lambda/2$ away from point P_1 at each frequency. The intersections of these curves give the values of βL corresponding to $5\beta_0 L = n\pi$ as can be seen by comparing Fig. 3 to Fig. 2. As shown by Fig. 3, the values at the edges of the pass bands are not included by this procedure. In this example, obviously, the reason at the lower edge is the difficulty of including the long wavelengths. At the

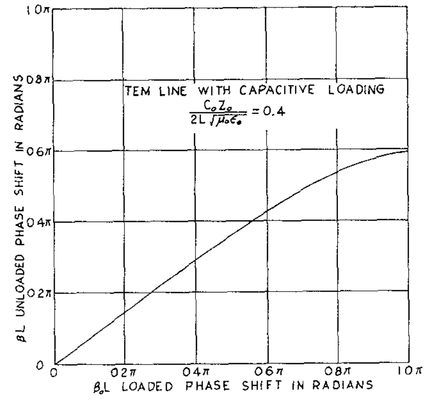

Fig. 2—Phase shift characteristics of a section of a periodic structure with loading elements spaced L distance apart.

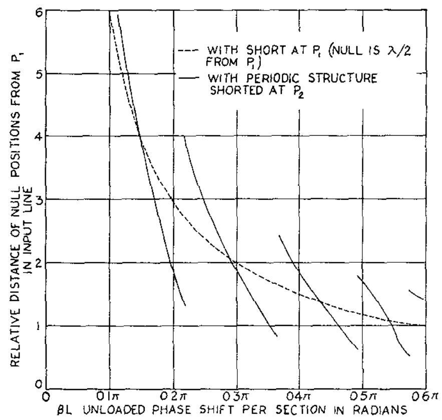

Fig 3—Calculated change of null positions in the input line as the frequency is varied ($\beta L = \omega L \sqrt{\mu_0 \epsilon_0}$).

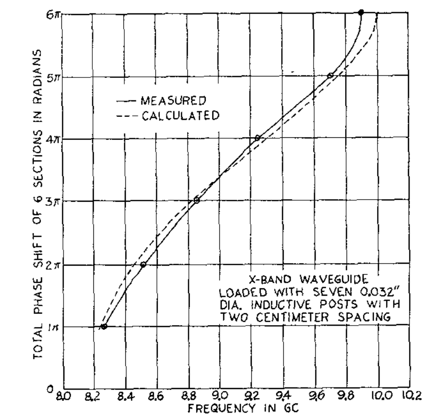

Fig. 4—Comparison of calculated phase shifts of a loaded waveguide with measured values obtained from the null movements.

upper edge, the reason is that the image impedance approaches an infinite value and (4) approaches a finite value instead of zero as might be expected from the tan $5\beta_0 L$ term. However, these edge-points can be located anyway from the knowledge of the pass band.

The application of this technique is not limited to the simple situation shown. For example, the characteristic impedance of the input line need not be the same as that of the loaded line so long as the reference nulls are located correctly. It is not necessary to have the $B_0/2$ matching sections at the end; the same results would be obtained if they were equal to B_0. Other types of loading can be handled as well as waveguide structures. Fig. 4 shows a comparison of experimental and calculated data for a structure consisting of seven 0.032-inch diameter inductive posts in the center of X-band waveguide (1 inch by $\frac{1}{2}$ inch outside dimensions) and spaced 2 cm apart. Although the exact shapes of the curves may vary depending on the actual situation, the technique can be applied to many periodic structures.

The efforts of S. N. James in constructing the circuit and making the measurements and calculations for Fig. 4 are gratefully acknowledged.

ODIS P. MCDUFF
Elec. Engrg. Dept.
University of Alabama
University, Ala

Synthetic Transmission-Line Impedance Transformers*

Somlo[1] has presented a convenient procedure for obtaining the characteristic impedance and length of a single section of lossless transmission line to match two impedances. One impedance and the conjugate of the other are plotted on a circular transmission-line chart, *i.e.*, Smith or Carter chart. A circle is drawn through the two points with its center on the $X = 0$ axis. If the circle does not lie entirely within the $R = 0$ circle, the two impedances cannot be matched with a single section of lossless transmission line with real characteristic impedance. However, if one does not require that the transmission line have a real characteristic impedance, it can be synthetized by a symmetrical T or π network consisting of either lossless inductances or capacitances.

A graphical procedure for obtaining the parameters of such a section of synthetic transmission line is presented here. The load impedance $\boldsymbol{Z_A}$ and the conjugate of the source impedance $\boldsymbol{Z_B}^*$ are plotted on a circular transmission-line chart, as shown in

* Received April 5, 1962.

[1] P. I. Somlo, "A logarithmic transmission line chart," IRE TRANS. ON MICROWAVE THEORY AND TECHNIQUES (*Correspondence*), vol. MTT-8, p. 463; July, 1960.

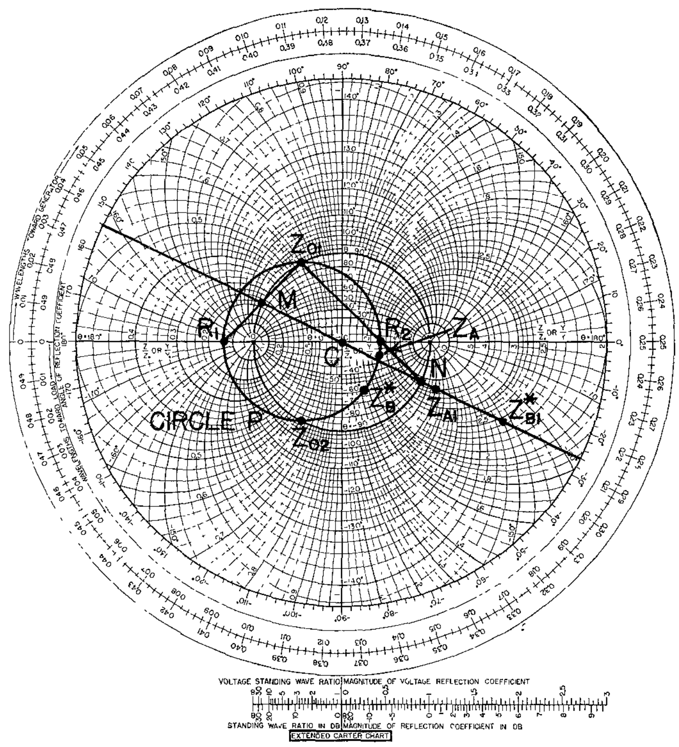

(a)

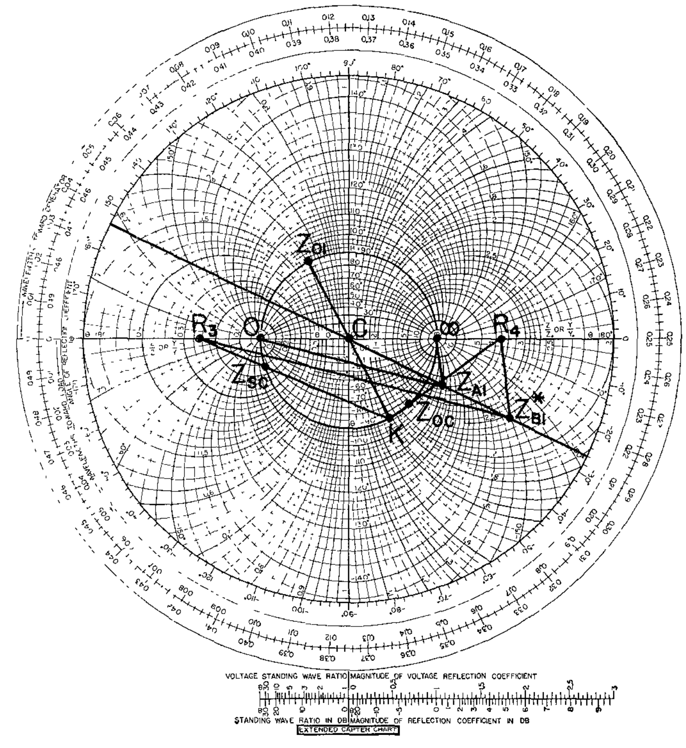

(b)

Fig. 1—Graphical construction.

Fig. 1. (Fig. 1 is in two parts to avoid crowding of lines and points.) An extended chart[2] is used because all points do not line on a conventional chart. The Carter chart is preferred over the Smith chart because less arithmetic is required.

The circle P is drawn through $\boldsymbol{Z}_A$ and $\boldsymbol{Z}_B^*$ with its center on the $\theta=0$ line. The two possible characteristic impedances of the transmission line are $\boldsymbol{Z}_{01}=+\sqrt{R_1\times R_2}$ and $\boldsymbol{Z}_{02}=-\sqrt{R_1\times R_2}$. The two values of $\boldsymbol{Z}_0$ are also given by the intersections of the circle P and the $\theta=\pm 90°$ circle. If $\boldsymbol{Z}_A$, $\boldsymbol{Z}_B^*$, and all other points on the circle P are normalized with respect to one of the possible values of $\boldsymbol{Z}_0$, say $\boldsymbol{Z}_{01}$, and replotted, they lie on a straight line through the center C of the chart.

The line $\boldsymbol{MN}$ onto which the circle P is mapped can be determined by drawing lines from $\boldsymbol{Z}_{01}$ through R_1 and R_2 to obtain the points of intersection $\boldsymbol{M}$ and $\boldsymbol{N}$ with the $\theta=\pm 90°$ circle. The point $\boldsymbol{Z}_{01}$ is mapped onto the point C, R_1 onto $\boldsymbol{M}$, R_2 onto $\boldsymbol{N}$, and $\boldsymbol{Z}_{02}$ onto $\boldsymbol{Z}=-1$, which is located at infinity. If a point lies on the circle P between $\boldsymbol{Z}_{01}$ and R_2, it is mapped onto a point inside the conventional chart, *i.e.*, within the $\theta=\pm 90°$ circle; otherwise, the point is mapped onto a point outside the $\theta=\pm 90°$ circle, *i.e.*, its resistive component is negative. The points $\boldsymbol{Z}_A$ and $\boldsymbol{Z}_B^*$ are mapped onto the points $\boldsymbol{Z}_{A1}$ and $\boldsymbol{Z}_{B1}^*$, respectively.

Let $\boldsymbol{\Gamma}_{A1}$ and $\boldsymbol{\Gamma}_{B1}^*$ denote the voltage reflection coefficients associated with $\boldsymbol{Z}_{A1}$ and $\boldsymbol{Z}_{B1}^*$, respectively. the ratio $\boldsymbol{\Gamma}_{B1}^*/\boldsymbol{\Gamma}_{A1}$ may be set equal to $\exp(-2\gamma l)$, where γ corresponds to the propagation constant and l corresponds to the length of a section of conventional transmission line. If the characteristic impedance of the transmission line is real and the line is lossless, γ is imaginary. However, in the case of the synthetic line, γ is real. In either case,

$$\boldsymbol{Z}_{SC} = \boldsymbol{Z}_0 \tanh \gamma l = \boldsymbol{Z}_0 \frac{1-\exp(-2\gamma l)}{1+\exp(-2\gamma l)}$$

and

$$\boldsymbol{Z}_{OC} = \boldsymbol{Z}_0 \coth \gamma l = \boldsymbol{Z}_0 \frac{1+\exp(-2\gamma l)}{1-\exp(-2\gamma l)}.$$

The values of $\boldsymbol{Z}_{SC}$ and $\boldsymbol{Z}_{OC}$ for the T or π network can be obtained graphically, as shown in Fig. 1(b). Draw lines from $\boldsymbol{Z}_{A1}$ to $\boldsymbol{Z}=0$ and $\boldsymbol{Z}=\infty$. Draw lines from $\boldsymbol{Z}_{B1}^*$ parallel to these lines to locate $R_3=\boldsymbol{Z}_{SC}/\boldsymbol{Z}_{01}$ and $R_4=\boldsymbol{Z}_{OC}/\boldsymbol{Z}_{01}$. Draw a line from $\boldsymbol{Z}_{01}$ through C to locate $\boldsymbol{K}=1/\boldsymbol{Z}_{01}$ on the $\theta=\pm 90°$ circle. Finally, draw lines from $\boldsymbol{K}$ through R_3 and R_4. The points of intersection with the $\theta=\pm 90°$ circle are $\boldsymbol{Z}_{SC}$ and $\boldsymbol{Z}_{OC}$.

For the construction shown in Fig. 1, $\boldsymbol{Z}_A=2.5\underline{/-20°}$, $\boldsymbol{Z}_B^*=1.5\underline{/-60°}$, $R_1=-0.142$, $R_2=2.643$, $\boldsymbol{Z}_{01}=-\boldsymbol{Z}_{02}=j0.612$, $\boldsymbol{M}=j0.231$, $\boldsymbol{N}=-j4.321$, $\boldsymbol{Z}_{A1}=4.087\underline{/-110°}$, $\boldsymbol{Z}_{B1}^*=2.452\underline{/-150°}$, $R_3=-0.264$, $R_4=-3.776$, $\boldsymbol{K}=-j1.635$, $\boldsymbol{Z}_{SC}=-j0.162$, and $\boldsymbol{Z}_{OC}=-j2.309$.

[2] H. F. Mathis, "Extended transmission-line charts," *Electronics*, vol. 33, pp. 76, 78; September 23, 1960.

It is interesting to consider what results might have been obtained if Z_{02} had been used as the characteristic impedance. In this case, the new values are $M=-j0.231$, $N=j4.321$, $Z_{A1}=4.087\underline{/70°}$, $Z_{B1}{}^{*}=2.452\underline{/30°}$, $K=j1.635$, $R_3=0.264$, $R_4=3.776$, $Z_{SC}=-j0.162$, and $Z_{OC}=-j2.309$. The same values of Z_{SC} and Z_{OC} are obtained in either case. In this case, all points lie on a conventional chart.

H. F. Mathis
Antenna Lab.
Dept. of Elec. Engrg.
The Ohio State University
Columbus, Ohio

A Unique Solid-State Diplexer*

A diplexer is a familiar device which readily combines two separate radio-frequency signals to permit simultaneous transmission through a single transmission line or separates a composite signal into its constituent parts to permit each part to be transmitted or proceed individually. This correspondence describes a unique method of deriving diplexing action in a simple Y-junction circulator, and suggests a method of diplexing in other devices which depend upon the phase shift properties of ferrimagnetic material for their operation.

The general properties of symmetrical junction circulators are well known. At most frequencies of interest a circulator can be made to operate in a condition such that the applied dc biasing field is either above or below ferrimagnetic resonance. The direction of signal flow from port to port around a circulator changes when the applied field is shifted from one side of resonance to the other.

Experiments were performed in our laboratory to determine the optimum frequency of operation and the dc biasing field required for operation at the optimum frequency in a circulator, both below and above resonance, for a series of aluminum substituted yttrium-iron garnets. Figs. 1 and 2 show how the frequency and field change as a function of $4\pi M_s$. Note that at a $4\pi M_s$ of 320 the same field is required for operation at the optimum frequency above resonance (5.5 Gc) as is required below resonance (7.4 Gc). Typical loss and isolation characteristics as a function of frequency are shown in Fig. 3. Fig. 4 depicts the operation of the device and how it can be used in the separation or combination of two signals. The isolation between channels was approximately 30 db and the loss was approximately 1 db. It seems likely that by using the same principle, that is simultaneous operation above and below resonance, a four-port phase shift type of duplexer (assuming broad-band microwave components) could be adapted, by the proper choice of geometry and ferrimagnetic material, to perform as a diplexer.

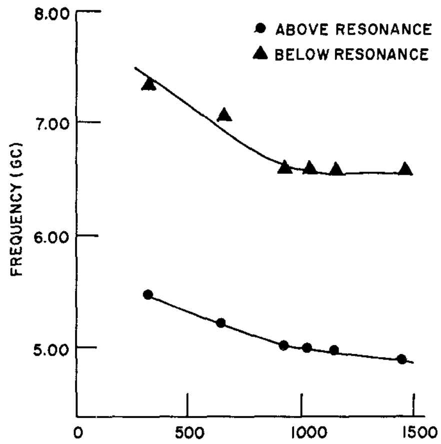

Fig. 1—Optimum frequency of operation for a series of aluminum substituted garnets.

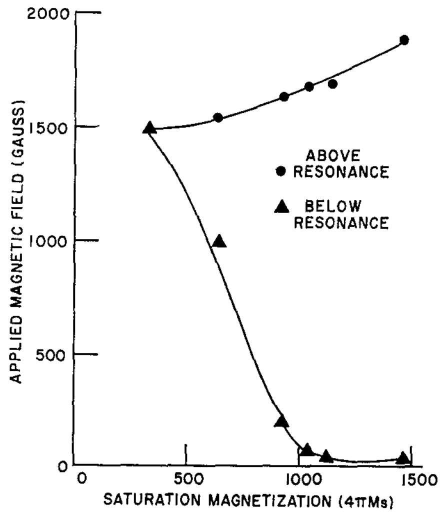

Fig. 2—Field required for operation at optimum frequency.

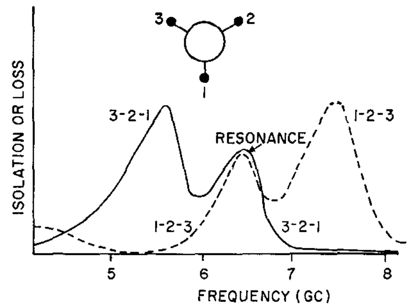

Fig. 3—Typical loss and isolation as a function of frequency.

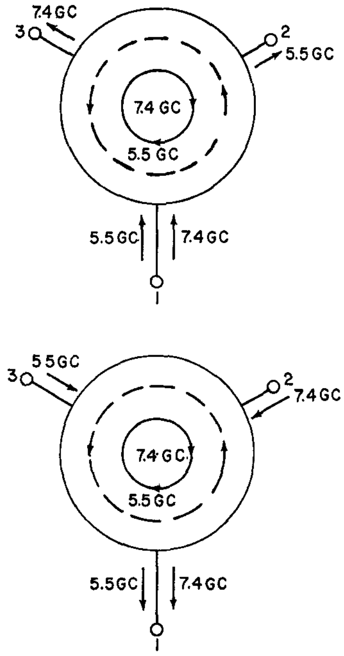

Fig. 4—Operation of a three-port circulator as a diplexer.

The authors are grateful to J. L. Allen who assisted in the preparation of the text and to D. E. Tribby who assisted with the laboratory measurements.

J. Brown
J. Clark
Solid State and Microwave Component Development Dept.
Sperry Microwave Electronics Co.
Clearwater, Fla.

* Received April 5, 1962.